A Note on the Mechanics of Ancient Gear Systems

F. Sorge*
University of Palermo
Palermo, Italy

Abstract—*This paper deals with the mechanical behavior of the gearwheels of the antiquity, which were generally characterized by triangular shaping of the teeth. The engagement of the conjugate profiles is analyzed in detail, calculating the temporal variation of the speed ratio due to the back and forth shifting of the relative instant center. The admissibility of the points of the theoretical contact path is carefully checked, estimating also the magnitude of the successive tooth collisions and ascertaining the energy losses arising from the particular nature of the coupling. Some very interesting results are that only one couple of teeth turns out to be active at each time instant and that the real path may belong to the only approach region or to the only recess region entirely or may be split into two separate sub-phases, the one in approach and the other in recess, or may even straddle both regions. The occurrence of each of these conditions depends on the average speed ratio (tooth ratio) and on the assigned clearance between the two wheels. It is also found that the speed oscillation is roughly contained in a ±10% range and the efficiency may reach rather high values, despite the presumable crude finishing of the ancient gearwheels due to the rudimentary technology used in the construction of the tooth profiles.*

Keywords: triangular tooth gearing, history of mechanics

I Introduction

Though only very few residues from the antiquity machinery are still preserved in some museums scattered over the world, it is legitimate to guess that a relatively advanced construction technology had been achieved and to imagine an extended practical use of many mechanical devices, especially in the Hellenistic, Byzantine and Islamic worlds.

The gearwheel coupling was no doubt a somehow current application and, for example, was largely used for the implementation of astronomical devices, like planetary calculators for the position of many celestial bodies, or astrolabes, or odometers.

One of the most significant find, the Antikythera mechanism (Fig. 1), is a planetary gear system, presumably of the first century B.C., ascribed perhaps to the philosopher Posidonius or to the astronomer Hypparchus of the Academy of Rhodes and used for the calculation of several astronomical positions. It was retrieved at the beginning of the XX century from the Antikythera wreck, which was accidentally discovered thanks to some sponge-divers anchored near the coast of the homonymous island (*Αντικύθηρα*, whose meaning is "in front of Kythera", is a very small Greek island with less than one hundred inhabitants in the sea channel between Crete and the larger island of Kythera).

Many in-depth studies have been carried out on its functionality as a primitive analog computer (for example, see Pastore [1], de Solla Price [2-3], Wright [4] and mind the recent activity of the Antikythera Mechanism Research Project [5]). Reference [1] by Pastore reports an extensive and careful description of this gear system and elucidates its functional characteristics. De Solla Price spent a lot of time in his studies about this mechanism, in order to reconstruct the missing parts starting from the few archeological residuals, and also tried to assemble a complete model, whose copy is now in the National Archaeological Museum of Athens. Wright carried out a wide campaign of X-ray detection of the wheel, continued later on by the Antikythera Mechanism Research Project, which pointed out the shape of equilateral triangles of the toothing unequivocally. On the other hand, it is sensational that such a profile denounces a less advanced design conception in comparison with the recent find of the gearwheel of Olbia (Sardinia, Italy), which may be ascribed to the genius of Archimedes of Syracuse (third century B.C.) and is then earlier than the Antikythera planetary of more than one century, but exhibits the extraordinary characteristic that the tooth profiles are very close to the modern cycloidal shape [1].

It is very probable that many gear systems like the Antikythera mechanism were built during the Hellenistic period. Cicero mentions two other devices of this type in *De Re Publica* and says that they had been built by Archimedes and one of them was brought to Rome by Marcus Claudius Marcellus, who conquered Syracuse during the Second Punic War. It is believed that the cycloidal gearwheel of Olbia belonged to one of these devices [1]. Cicero also says that another such device had been built "recently" by a friend of him and thus, this technology was quite spread since the time of Archimedes and the Antikythera orrery was only one exemplar of a widely diffused manufacturing, though skilled hands and complex calculations were needed for this type of construction.

* francesco.sorge@unipa.it

Fig. 1. Main fragment of the Antikythera mechanism at the National Archaeological Museum of Athens.

The complex technology needed for the construction of these gear systems was transmitted, through the Hellenistic world, to the Byzantine and Islamic culture and gave the conceptual origin to several geared machines in the Middle Age, like odometers, mechanical calendars and clockworks (for example, bear in mind some machines described in the books of the Byzantine monasteries, the volume Kitab al-Hiyal by Banu Musa, the odometers and astrolabes of al Biruni, etc.).

We can also find gear devices in the codices of Leonardo da Vinci, i. e. at the dawn of the Modern Era. However, the tooth shape is still quite rudimentary, often triangular, and far from the modern cycloidal or involute profiles developed after Euler.

The present analysis aims at stating the fundamentals of the mechanical coupling of ancient triangular gears. There seems to be no previous study of this type.

II. Geometry of triangular toothed gears

A scheme of the gear coupling is represented in Fig. 2 a, b and c for three possible contact configurations: approach, profile matching and recess. The sizes are chosen in accordance to the design concepts to be presumed for those ancient times. Some elementary constraints lead to forced choices of the system data (constant pitch, equal tooth depth, etc.), while other variables are assumed *ad lib*.

The ratio of the tooth numbers of the two gears corresponds to the average speed ratio, which is imposed by the machine employment, though the simple geometrical shape of the tooth profiles implies the variability of the instant speed ratio during the meshing.

It is supposed firstly that each couple of conjugate teeth engages along the whole ideal path, ignoring the possible restrictions involved by the presence of the preceding and following teeth. In actual fact, the number of active teeth and the true line of contact for sequential tooth gearings is limited by the need of avoiding interference conditions and will be examined in the following Section III *C*.

It is assumed that the teeth on the one and the other gear have the same aperture angle 2β and the same depth h from the vertex V to the root circle, whence, fixing the tooth numbers, the whole toothing can be designed relying on evident geometrical considerations.

The triangle OBV in the detail on the lower side of Fig. 2 shows that the tooth depth h and the side profile width e are calculable as

$$h = R\left[1 - \frac{\sin\beta}{\sin\left(\beta + \frac{\pi}{z}\right)}\right] \tag{1}$$

$$e = R\frac{\sin\frac{\pi}{z}}{\sin\left(\beta + \frac{\pi}{z}\right)} \tag{2}$$

for each gearwheel, where R and $R - h$ are the tip and root radii and z is the tooth number.

Thus, the assumption of equal depths permits writing

$$\frac{R_2}{R_1} = \frac{1 - \frac{\sin\beta}{\sin\left(\beta + \frac{\pi}{z_1}\right)}}{1 - \frac{\sin\beta}{\sin\left(\beta + \frac{\pi}{z_2}\right)}} \tag{3}$$

and calculating for example R_2 once fixed R_1.

The minimum value of the center distance D is $D_{\min.} = R_1 + R_2 - h$, but a tolerance factor a, a little greater than 1, has to be multiplied by $D_{\min.}$ necessarily in order to consider some backlash, which was especially needed in the antiquity to let the gear system work, in consideration of the unavoidable manufacturing inaccuracy because of the crude technology of those days. Thus, $D = aD_{\min.}$.

After fixing D, the ideal angular width of the meshing region is specified by the intersections of the two tip circumferences, of radii R_1 and R_2:

$$\cos\alpha_{i\max.} = \frac{D^2 + R_i^2 - R_j^2}{2DR_i} \tag{4}$$

where i and j may stand either for 1 and 2 or for 2 and 1, while α_i indicates the generic angular position of the

gearwheel *i*, which is positive or negative for the meshing entrance or exit of both wheels, according to Fig. 2.

III. Kinematics of the gear coupling

Refer to Fig. 2 for the notation throughout the present section.

Starting from the initial meshing point on the first intersection of the two tip circles, where the two teeth are in contact through the apices, there is a first phase, where the apex of the driven tooth is pushed and slides along the side of the driver tooth, and a second phase, where the driver tooth apex pushes the side of the driven tooth, as far as the ending meshing point, on the second intersection of the tip circles. Such two phases are separated by the matching position of the two profiles, which occurs for $-\alpha_2 = \alpha_1$. This matching value will be called α_{1m} and the two phases will be named of approach and recess, though somehow improperly if comparing with the modern gear terminology.

Thus, the approach contact locus coincides with the arc of the driven tip circle preceding the matching position α_{2m} (< 0) and the recess contact locus with the arc of the driver tip circle following the matching position α_{1m} (> 0). The instant center of the relative motion is given by the intersection of the normal to the active profile, of the driver wheel in approach (n_a) and of the driven one in recess (n_r), and the center line. A sudden change of the speed ratio must occur when passing from the matching position of the two teeth.

In dependence on α_1, it is possible to calculate the driven angle α_2 and the distance $v = \overline{V_1V_2}$ between the two vertices by use of specific closure equations, different for the approach and the recess.

A. Approach phase

Apply the two closure equations

$$R_1\cos\alpha_1 - v\cos(\alpha_1+\beta) + R_2\cos\alpha_2 = D \qquad (5)$$

$$R_1\sin\alpha_1 - v\sin(\alpha_1+\beta) - R_2\sin\alpha_2 = 0 \qquad (6)$$

to get, by elimination of *v*,

$$\alpha_2(\alpha_1) = \arcsin\left[\frac{D\sin(\alpha_1+\beta) - R_1\sin\beta}{R_2}\right] - \alpha_1 - \beta \qquad (7)$$

Then, calculating $\cos\alpha_2$ and $\sin\alpha_2$ by Eqs. (5-6), squaring and summing, α_2 is easily eliminated and we get a quadratic equation for *v*,

$$\begin{aligned} v^2 + 2v\left[D\cos(\alpha_1+\beta) - R_1\cos\beta\right] + \\ + \left[\left(D^2 + R_1^2 - 2DR_1\cos\alpha_1\right) - R_2^2\right] = 0 \end{aligned} \qquad (8)$$

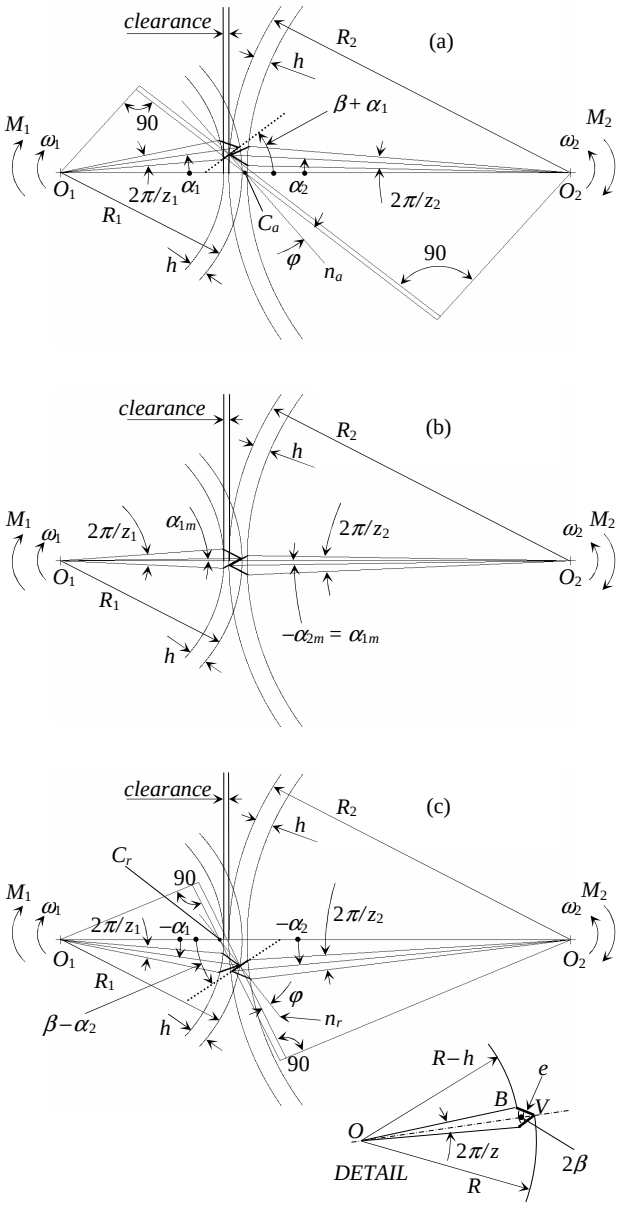

Fig. 2 a, b, c. Scheme of tooth coupling. $z_2/z_1 = 2$, $\beta = 30°$.
a) approach phase; b) profile matching; c) recess phase

where the coefficient of the linear term is equal to twice the positive difference of the projections of *D* and R_1 on the straight line containing the diver profile, while the third term is equal to $\overline{O_2V_1}^2 - R_2^2$ and is negative as V_1 is inside the driven tip circle. These observations address the choice between the two roots of Eq. (8) towards the plus sign,

$$\begin{aligned} v(\alpha_1) = R_1\cos\beta - D\cos(\alpha_1+\beta) + \\ + \sqrt{R_2^2 - \left[D\sin(\alpha_1+\beta) - R_1\sin\beta\right]^2} \end{aligned} \qquad (9)$$

and it may be noticed that the term under the square root is equal to the projection of the tip radius R_2 on the straight line of the driver profile.

The approach phase ends when $\alpha_2 = -\alpha_1$ ($\alpha_1 = \alpha_{1m}$), whence we get by Eq. (7):

$$\alpha_{1m} = \arcsin\left[\frac{(R_1 + R_2)\sin\beta}{D}\right] - \beta \tag{10}$$

The instant center C_a of the relative motion is found on the center line, tracing the normal n_a to the driver tooth profile, whose slope is equal to $\pi/2 - \alpha_1 - \beta$. Equating the projections of $\overline{O_2C_a}$ and $\overline{O_2V_2}$ on the prolongation of the driver profile, the distance $\overline{O_2C_a}$ is found to be

$$\overline{O_2C_a} = \frac{\sqrt{R_2^2 - [D\sin(\alpha_1+\beta) - R_1\sin\beta]^2}}{\cos(\alpha_1+\beta)} \tag{11}$$

whence the speed ratio $\tau = \omega_2/\omega_1 = \overline{O_1C_a}/\overline{O_2C_a} = D/\overline{O_2C_a} - 1$ is obtainable as

$$\tau(\alpha_1) = \frac{D\cos(\alpha_1+\beta)}{\sqrt{R_2^2 - [D\sin(\alpha_1+\beta) - R_1\sin\beta]^2}} - 1 \tag{12}$$

B. Recess phase

After passing the matching configuration, the apex of the driver tooth slides on the driven tooth side, whose slope is $\beta - \alpha_2$, and the two closure equations are

$$R_1\cos\alpha_1 - v\cos(\beta-\alpha_2) + R_2\cos\alpha_2 = D \tag{13}$$

$$R_1\sin\alpha_1 - v\sin(\beta-\alpha_2) - R_2\sin\alpha_2 = 0 \tag{14}$$

As it is desired to express all variables as functions of α_1, the distance v may be firstly calculated, solving Eqs. (13-14) for $\cos\alpha_2$ and $\sin\alpha_2$, squaring and summing

$$v^2 - 2vR_2\cos\beta + \left[R_2^2 - \left(D^2 + R_1^2 - 2DR_1\cos\alpha_1\right)\right] = 0 \tag{15}$$

where the third term is equal to $R_2^2 - \overline{O_2V_1}^2$ and is positive, so that both roots of Eq. (15) are positive. Nevertheless, the geometric meaning of Eq. (15) is that, fixing the angular position α_1 of the vertex V_1, which is inside the circumference of radius R_2, one has to find the position of point V_2 on this last circumference so that the angle $V_1\hat{V}_2O_2$ is equal to β. Two possible positions fulfill this condition, but the one closest to V_1 is clearly to be selected, i. e. the lowest root v:

$$v(\alpha_1) = R_2\cos\beta + \sqrt{\left(D^2 + R_1^2 - 2DR_1\cos\alpha_1\right) - R_2^2\sin^2\beta} \tag{16}$$

Since $D^2 + R_1^2 - 2DR_1\cos\alpha_1 = \overline{O_2V_1}^2$, since $R_2\sin\beta$ gives the minimum distance of the centre O_2 from the straight line prolonging the side of the driven tooth and since the apex V_1 lies on this line, the quarter-discriminant under square root of Eq. (16) is certainly positive.

After obtaining v, it is possible to get α_2 by back calculation

$$\alpha_2(\alpha_1) = \arctan\left[\frac{\left(\frac{R_1\sin\alpha_1}{D - R_1\cos\alpha_1}\right) - \left(\frac{v\sin\beta}{R_2 - v\cos\beta}\right)}{1 + \left(\frac{R_1\sin\alpha_1}{D - R_1\cos\alpha_1}\right)\left(\frac{v\sin\beta}{R_2 - v\cos\beta}\right)}\right] \tag{17}$$

and Equation (17) may be observed to be equivalent to stating that the absolute value of α_2 is given by the sum of the angles formed by $\overline{O_2V_1}$ with the center line and with the radius $\overline{O_2V_2}$.

The instant center C_r of the relative motion during the recess phase is located on the center line, on the intersection with the normal n_r to the driven tooth profile, whose slope is equal to $\pi/2 - \beta + \alpha_2$. Equating the projections of $\overline{O_1C_r}$ and $\overline{O_1V_1}$ along the direction parallel to the driven profile, the distance $\overline{O_1C_r}$ is given by

$$\overline{O_1C_r} = \frac{R_1\cos(\beta - \alpha_1 - \alpha_2)}{\cos(\beta - \alpha_2)} \tag{18}$$

and the speed ratio $\tau = \omega_2/\omega_1$ is

$$\tau(\alpha_1) = \frac{R_1\cos(\beta - \alpha_1 - \alpha_2)}{D\cos(\beta - \alpha_2) - R_1\cos(\beta - \alpha_1 - \alpha_2)} \tag{19}$$

where $\alpha_2(\alpha_1)$ is given by Eq. (17).

C. Real meshing conditions

Of course, the teeth are closely distributed in two regular sequences, on the one and the other wheel, and, after ascertaining that the contact conditions cannot but be described by the analysis of the previous subsections, it is necessary to investigate if all the ideal contact points are admissible and if several meshing couples may be in contact simultaneously.

Choosing a generic contact point on the ideal path, either in approach or in recess, the homologous points of the preceding or following tooth couples have angular distances $\pm 2\pi j/z_1$ and $\pm 2\pi j/z_2$ in the driver and driven gearwheels respectively, where j = 1, 2, … Therefore,

drawing the full ideal diagram $\alpha_2(\alpha_1)$ a generic point must be regarded as admissible only if, tracing a straight line with slope z_1/z_2 through such a point, all the other points whose abscissae differ of $\pm 2\pi j/z_1$ from it lie below the diagram, as otherwise there would be interference for some tooth couple.

Since the diagram $\alpha_2(\alpha_1)$ will be shown to exhibit a slight upward concavity nearly everywhere except at the matching position α_{1m}, where a sudden slope change occurs, the above reasoning leads to exclude all points of the diagram that lie above the prolongation of that particular chord (or sum of aligned chords) with slope z_1/z_2 and (total) projection $2\pi j/z_1$ on the α_1 axis, that is located as much as possible at the bottom of the main concavity. The admissible contact points, which must lie below this straight line, may then be searched by checking the interference condition of the preceding and following teeth at any position of the ideal path.

The consequence is in practice that only one couple of profile may be in contact at each time instant and, as soon as such profiles detach themselves, two new profiles, either of the following or of the preceding tooth couple, join simultaneously to mesh, either upstream or downstream. This will be better elucidated by showing some practical results from the numerical calculations.

On the other hand, comparing with the inverse motion, it may be proven that the back inactive profiles of the teeth are quite far from the interference condition.

D. Tooth collision

The motion transmission is continuous, but the speed ratio is variable, as the position of the instant center of the relative motion moves back and forth along the center line. Moreover, since the entrance speed ratio is always a little higher than the exit one, because the relative instant center shifts towards the driver wheel center during each partial engagement, a slight impact occurs at the beginning of any mesh phase or sub-phase, as the driven profile has a slightly lower speed before the engagement than after it.

It is supposed that the impact is inelastic, so that, immediately after the conjunction of two profiles, the velocity components of the driver and driven point along the normal to the contact are equal, while immediately before this instant, the driven velocity component is smaller, where the difference is proportional to the speed ratio jump.

The velocity components normal to the active profiles may be obtained as the total velocities of those points of the two planes rotating rigidly with the one and the other wheel, that are located on the intersections of the parallels to the profile traced from the wheel centers with the normal to the profile itself.

It will be shown that, for not too large backlash, the meshing phase is entirely in the approach region for z_1/z_2 rather larger than 1 and in the recess one for z_1/z_2 rather smaller than 1. On the contrary, in the neighborhood of $z_1/z_2 = 1$, we may observe two sub-phases, the one in approach and the other in recess, distant one angular pitch from each other and with a trend to join into a single phase on increasing the backlash. On the other hand, whatever the tooth ratio may be, the meshing phase tends to straddle the approach and recess regions on increasing the backlash, as is also intuitive.

If the whole meshing phase is in the approach region, indicating the driver and driven angular speeds with ω_1 and $\omega_2 = \tau\omega_1$, the velocity components normal to the active (driver) profile are

$$\begin{aligned} v_{1\perp} &= \omega_1 \overline{O_1 C_a} \cos(\beta+\alpha_1) = \\ &= \omega_1 \left\{ D\cos(\beta+\alpha_1) - \sqrt{R_2^2 - [D\sin(\beta+\alpha_1) - R_1\sin\beta]^2} \right\} \end{aligned} \tag{20}$$

$$\begin{aligned} v_{2\perp} &= \tau\omega_1 R_2 \cos(\beta+\alpha_1+\alpha_2) = \\ &= \tau\omega_1 \sqrt{R_2^2 - [D\sin(\beta+\alpha_1) - R_1\sin\beta]^2} \end{aligned} \tag{21}$$

Indicating the conditions preceding and following the impact with the superscripts – and + respectively and assuming for example that ω_1 is constant, one has $v_{1\perp}^- = v_{1\perp}^+ = v_{1\perp}$ and $v_{2\perp}^+ = v_{1\perp}$, whence $v_{2\perp}^-/v_{1\perp} = v_{2\perp}^-/v_{2\perp}^+ = \tau^-/\tau^+$, so that $(v_{2\perp}^+ - v_{2\perp}^-) / v_{1\perp} = 1 - \tau^-/\tau^+$ and, calculating the speed ratios at the beginning and the end of the meshing phase by Eq. (12), one obtains

$$\frac{v_{2\perp}^+ - v_{2\perp}^-}{v_{1\perp}} = 1 - \frac{\dfrac{D\cos(\beta+\alpha_{1e})}{\sqrt{R_2^2 - [D\sin(\beta+\alpha_{1e}) - R_1\sin\beta]^2}} - 1}{\dfrac{D\cos(\beta+\alpha_{1i})}{\sqrt{R_2^2 - [D\sin(\beta+\alpha_{1i}) - R_1\sin\beta]^2}} - 1} \tag{22}$$

where the subscripts *i* and *e* define the initial and ending values of the angle α_1.

When the whole meshing occurs in the recess region, the velocity components normal to the active (driven) profile are

$$v_{1\perp} = \omega_1 R_1 \cos(\beta - \alpha_1 - \alpha_2) \tag{23}$$

$$\begin{aligned} v_{2\perp} &= \tau\omega_1 \overline{O_2 C_r} \cos(\beta - \alpha_2) = \\ &= \tau\omega_1 [D\cos(\beta - \alpha_2) - R_1 \cos(\beta - \alpha_1 - \alpha_2)] \end{aligned} \tag{24}$$

Proceeding as in the previous case, but using now Eq. (19), one gets

$$\frac{v_{2\perp}^+ - v_{2\perp}^-}{v_{1\perp}} = 1 - \frac{\dfrac{D\cos(\beta-\alpha_{2i})}{\cos(\beta-\alpha_{1i}-\alpha_{2i})} - R_1}{\dfrac{D\cos(\beta-\alpha_{2e})}{\cos(\beta-\alpha_{1e}-\alpha_{2e})} - R_1} \tag{25}$$

If the meshing begins in the approach region and ends in the recess one, which may occurs for large clearances, it is possible to use both equations Eqs. (12) and (19), minding that the initial speed ratio refers to the approach and the ending one to the recess:

$$\frac{v_{2\perp}^{+}-v_{2\perp}^{-}}{v_{1\perp}}=1-\frac{\dfrac{R_1\cos(\beta-\alpha_{1e}-\alpha_{2e})}{D\cos(\beta-\alpha_{2e})-R_1\cos(\beta-\alpha_{1e}-\alpha_{2e})}}{\dfrac{D\cos(\beta+\alpha_{1i})}{\sqrt{R_2^2-[D\sin(\beta+\alpha_{1i})-R_1\sin\beta]^2}}-1} \quad (26)$$

At last, if the meshing phase splits into two sub-phases, the one in the approach region and the other in the recess one, their total width and the distance between each other are both equal to the angular pitch (see Section V). Therefore, each couple of profiles starts the engagement in the approach region and meshes for a period shorter than the angular pitch, at whose end the preceding couple engages in the recess region and meshes for the complementary angular pitch, until separating simultaneously with the engagement of the new couple of profiles, following the first one, in the approach region. For the impact at the beginning of the approach sub-phase, Equation (26) may be used, choosing properly τ_e (end of the preceding recess sub-phase), while for the starting impact of the recess sub-phase, one has to use an inverse relationship with respect to Eq. (26), minding that τ_e refers now to the end of the preceding approach sub-phase:

$$\frac{v_{2\perp}^{+}-v_{2\perp}^{-}}{v_{1\perp}}=1-\frac{\dfrac{D\cos(\beta+\alpha_{1e})}{\sqrt{R_2^2-[D\sin(\beta+\alpha_{1e})-R_1\sin\beta]^2}}-1}{\dfrac{R_1\cos(\beta-\alpha_{1i}-\alpha_{2i})}{D\cos(\beta-\alpha_{2i})-R_1\cos(\beta-\alpha_{1i}-\alpha_{2i})}} \quad (27)$$

Likewise, in the particular case when the engagement straddles both, approach and recess regions, in addition to the impact described by Eq. (26), also the impact of the tooth profiles at the matching position must be taken into account. All the intermediate points of the driven profile between the two tooth tips bounce on the driver profile, except the inner point, which remains in contact, and the velocity jump is still given by Eq. (27), provided that one replaces α_{1i} and α_{1e} with α_{1m}, and α_{2i} with $-\alpha_{1m}$.

All these impacts involve relative speed jumps up to the order of 10% and may produce a significant rattle of the gear system if the driving crank has an appreciable angular speed.

IV. Power loss

Apart from the other energy losses, for example in the supports, or because of the air drag, or because of other loss sources, the losses to be ascribed to the tooth meshing are due to the sliding friction and to the tooth impact.

The ideal pressure angle, formed by the normals to the active profile and to the center line, is $\beta + \alpha_1$ in the approach phase and $\beta - \alpha_2$ in the recess one and is quite larger in comparison with the modern involute toothing.

Owing to the sliding friction, the line of action of the force exerted by the driver tooth on the driven one is rotated of the friction angle $\varphi = \arctan f$ with respect to the normal, towards the center of the driven wheel, both in the approach and in the recess phases (see Fig. 2).

Since only one couple of teeth is active at each time instant, the problem is isostatic and the mutual force is given by the ratio of the driver torque M_1, which is assumed constant, except the instantaneous peaks due to the tooth collisions, and the corresponding arm b_1. Tracing the parallel to the line of action of the mutual force through the relative instant center as in Fig. 2, the arms b_1 and b_2 are calculable as $b_1 = \overline{O_1C_a}\cos(\beta+\alpha_1+\varphi_2) + \overline{V_2C_a}\sin\varphi$, $b_2 = \overline{O_2C_a}\cos(\beta+\alpha_1+\varphi_2) - \overline{V_2C_a}\sin\varphi$, for an approach contact, and $b_1 = \overline{O_1C_r}\cos(\beta-\alpha_2+\varphi_1) + \overline{V_1C_r}\sin\varphi$, $b_2 = \overline{O_2C_r}\cos(\beta-\alpha_2+\varphi_1) - \overline{V_1C_r}\sin\varphi$, for a recess one, where $\varphi_1 = \varphi\,\mathrm{sgn}(\alpha_1)$, $\varphi_2 = \varphi\,\mathrm{sgn}(\alpha_2)$. Considering that $\overline{V_2C_a} = R_2|\sin\alpha_2|/\cos(\beta+\alpha_1)$, $\overline{V_1C_r} = R_1|\sin\alpha_1|/\cos(\beta-\alpha_2)$, $\overline{O_1C} = \tau\,\overline{O_2C}$, using Eqs. (11) and (18) and carrying out some calculations, the values of b_1 and b_2 are found to be given by

$$b_1=\frac{R_2[\tau\cos(\beta+\alpha_1+\alpha_2)\cos(\beta+\alpha_1+\varphi_2)+\sin\alpha_2\sin\varphi_2]}{\cos(\beta+\alpha_1)} \quad (28)$$

$$b_2=\frac{R_2[\cos(\beta+\alpha_1+\alpha_2)\cos(\beta+\alpha_1+\varphi_2)-\sin\alpha_2\sin\varphi_2]}{\cos(\beta+\alpha_1)} \quad (29)$$

during the approach, and

$$b_1=\frac{R_1[\cos(\beta-\alpha_1-\alpha_2)\cos(\beta-\alpha_2+\varphi_1)+\sin\alpha_1\sin\varphi_1]}{\cos(\beta-\alpha_2)} \quad (30)$$

$$b_2=\frac{R_1\left[\dfrac{\cos(\beta-\alpha_1-\alpha_2)\cos(\beta-\alpha_2+\varphi_1)}{\tau}-\sin\alpha_1\sin\varphi_1\right]}{\cos(\beta-\alpha_2)} \quad (31)$$

during the recess.

The efficiency η_f due to the only sliding friction is obtainable as the product of the speed ratio τ and the arm ratio b_2/b_1:

$$\eta_{f,\mathrm{access}}=\frac{\cos(\beta+\alpha_1+\alpha_2)\cos(\beta+\alpha_1+\varphi_2)-\sin\alpha_2\sin\varphi_2}{\cos(\beta+\alpha_1+\alpha_2)\cos(\beta+\alpha_1+\varphi_2)+\dfrac{\sin\alpha_2\sin\varphi_2}{\tau}} \quad (32)$$

$$\eta_{f,\mathrm{recess}}=\frac{\cos(\beta-\alpha_1-\alpha_2)\cos(\beta-\alpha_2+\varphi_1)+\tau\sin\alpha_1\sin\varphi_1}{\cos(\beta-\alpha_1-\alpha_2)\cos(\beta-\alpha_2+\varphi_1)-\sin\alpha_1\sin\varphi_1} \quad (33)$$

The sliding friction energy loss during one complete meshing of two conjugate teeth can be calculated by integration:

$$L_f = \int_{\Delta\alpha_{1,\mathrm{tot}}} (1-\eta_f) M_1 d\alpha_1 \qquad (34)$$

where, in the case of two partial contact sub-regions, the integration must be extended to both of them. The torque applied to the driven gearwheel is $M_1 b_2/b_1$ and is variable owing to the variability of the arms b_1 and b_2. Furthermore, this torque differs from the output resistant torque due to the secondary shaft inertia and the variability of ω_2.

As regards the impact losses, the previous assumptions of constancy of the driving speed ω_1 and inelastic impacts lead to the conclusion that, for every tooth collision, the work $\frac{1}{2} J_2 \omega_1^2 (\tau_i^{2+} - \tau_i^{2-})$ must be provided by the driving wheel, where J_2 indicates the moment of inertia of the driven wheel and all the masses connected to the driven shaft, while the speed ratios τ refer to the instants immediately after and before the impact, to be calculated as in the previous section. In the case of two partial contact sub-region or of one single region astride the matching position, two impact works must be taken into account, because of the approach, recess and matching impact. Such impact works have to be added to the sliding friction work, Eq. (34), to get the total lost energy due to the tooth coupling during one single mesh.

V. Results

Figures 3 to 5 show the numerical results arising from the above formulation for three tooth ratios z_2/z_1 and two values of the clearance factor $a = D/(R_1 + R_2 - h)$.

Figures 3 a and b refer to a speed down case. The active fraction of the diagram is confined in the recess region and its width along the abscissa axis is $360°/z_1$. The concavity of the diagram $\alpha_2(\alpha_1)$ is slight and upward directed, so that the admissible active points are confined under the bottom chord of width $360°/z_1$ and slope z_1/z_2.

The speed ratio decreases along the direction of the meshing evolution, i. e. from right to left.

Close to the matching position, α_{1m}, the distance of the contact point from the relative rotation center C is very small, which justifies the high sliding efficiency near this position. A coefficient of friction $f = 0.2$ was chosen in all the examples, assuming bronze gearwheels and some sort of rudimentary lubrication, which compensates for the necessarily crude profile finishing somehow.

Comparing Fig. 3 a with Fig. 3 b, which refers to a larger backlash, it is possible to observe a significant reduction of the ideal meshing width, but no remarkable changes in the real mesh. Therefore, rather large

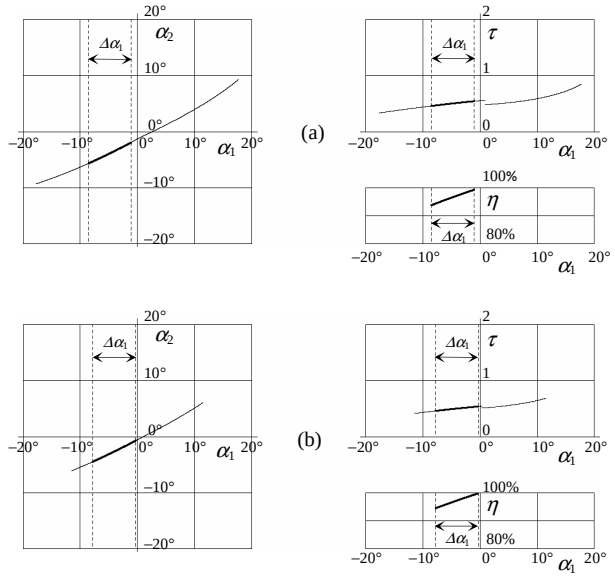

Fig. 3 a, b. Secondary rotation α_2, speed ratio τ and sliding efficiency η, in dependence on the driver gearwheel rotation α_1. $\Delta\alpha_1 = 360/z_1$. $z_1 = 48$, $z_2 = 96$, $\beta = 30°$, $f = 0.2$.
(thicker line: admissible working points without interference).
(a) clearance factor $a = 1.01$, $\Delta v_{2\perp}/v_{1\perp} = 0.1582$, $\tau_{\mathrm{mean}} = 0.5000$;
(b) clearance factor $a = 1.025$, $\Delta v_{2\perp}/v_{1\perp} = 0.1457$, $\tau_{\mathrm{mean}} = 0.5000$.

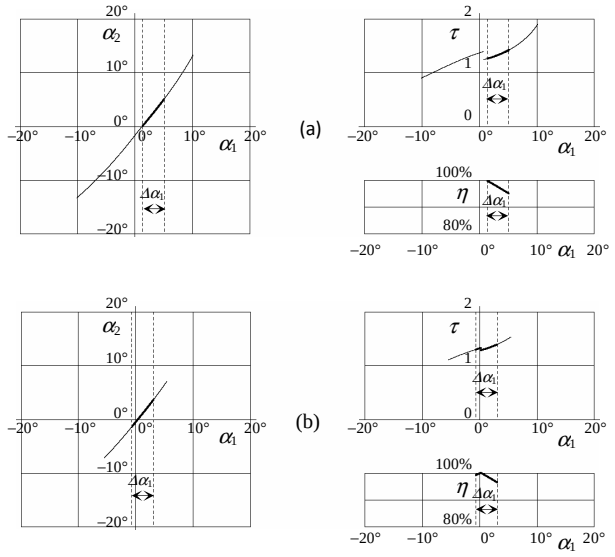

Fig. 4 a, b. Secondary rotation α_2, speed ratio τ and sliding efficiency η, in dependence on the driver gearwheel rotation α_1. $\Delta\alpha_1 = 360/z_1$. $z_1 = 96$, $z_2 = 72$, $\beta = 30°$, $f = 0.2$.
(thicker line: admissible working points without interference).
(a) clearance factor $a = 1.01$, $\Delta v_{2\perp}/v_{1\perp} = 0.1117$, $\tau_{\mathrm{mean}} = 1.3333$;
(b) clearance factor $a = 1.025$, $(\Delta v_{2\perp}/v_{1\perp})_a = 0.0682$, $(\Delta v_{2\perp}/v_{1\perp})_m = 0.0314$, $\tau_{\mathrm{mean}} = 1.3333$.

clearances can be adopted without any important worsening of the mesh conditions, to the advantage of the

prevention of possible transmission stops due to the tooth locking.

Figures 4 a and b refer to a speed up case and similar comments can be made as for Figs. 3. The main difference is that the real mesh phase develops inside the approach region, but tends to develop astride the matching position on increasing the backlash. This last feature is clearly typical of all cases.

Figures 5 a and b refer to a unitary speed ratio. For small clearance, two partial meshing regions can be observed, the one in the approach region and the other in the recess one. The sum of the widths of these two sub-regions along the α_1 axis is equal to $360°/z_1$ and is also equal to the distance between them. Therefore, indicating with the numbering, $j - 1$, j, $j + 1$, the sequence of three successive couples of conjugate teeth and starting the analysis of the engagement with the approach sub-phase of the couple j, from the right of the diagram towards the central position, the couple $j - 1$ begins the engagement of the other sub-phase, in the recess region, immediately after the conclusion of the approach sub-phase of j, and keeps on until this recess sub-phase is entirely covered. Then, the couple $j + 1$ starts a new approach sub-phase from the right end and the whole process begins again. This sequence is permitted by the circumstance that the distance between the two extremes endpoints, on the right of the approach contact and on the left of the recess contact, is exactly equal to $2\times360°/z_1$.

On increasing the clearance, the left sub-region width decreases to the advantage of the right one, their total width and their mutual distance remaining unchanged, until it vanishes and leaves only one single contact region. On increasing the clearance further, this unique phase moves to the left, until straddling the matching configuration α_{1m} and lying in part in the approach region and in part in the recess one. This is clearly visible in the case of Fig. 5 b, where the sliding efficiency reaches its highest average value and the impact velocity jump $v_{2\perp}^{+} - v_{2\perp}^{-}$ is very low. For this configuration, i. e. speed ratio 1:1 and rather large backlash, we get thus the best conditions as regards the energy losses. Clearly the gearwheel clearance cannot be increased too much because, if the ideal region of virtual contact becomes smaller than $360°/z_1$, we may have standstill period of the driven wheel, with important collisions at the new motion start, or else its definitive arrest.

VI. Conclusion

The extraordinary advancement degree of the Hellenistic science in conceiving planetary gear systems is somehow overshadowed by the technology primitiveness of that time. Nevertheless, an appreciable level of functionality can be detected by an accurate analysis. The gearing behavior was certainly

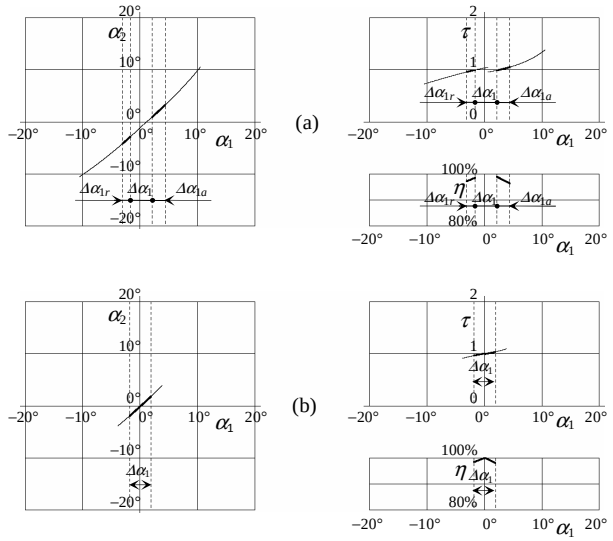

Fig. 5 a, b. Secondary rotation α_2, speed ratio τ and sliding efficiency η, in dependence on the driver gearwheel rotation α_1. $\Delta\alpha_1 = 360°/z_1$. $z_1 = 96$, $z_2 = 96$, $\beta = 30°$, $f = 0.2$.
(thicker line: admissible working points without interference).
(a) clearance factor $a = 1.01$, $(\Delta v_{2\perp}/v_{1\perp})_a = 0.0876$, $(\Delta v_{2\perp}/v_{1\perp})_r = 0.0095$, $\tau_{mean} = 1.0000$, $\Delta\alpha_{1a} + \Delta\alpha_{1r} = 360°/z_1$;
(b) clearance factor $a = 1.025$, $(\Delta v_{2\perp}/v_{1\perp})_a = 0.0696$, $(\Delta v_{2\perp}/v_{1\perp})_m = 0.0119$, $\tau_{mean} = 1.0000$.

characterized by a sensible rattling noise due to the tooth collisions consequent to the variability of the speed ratio. The energy losses were of course more relevant in comparison with the present gear systems, but, guessing that a sort of rudimentary greasing or oiling of the contact might have been applied even in the antiquity, the friction losses due to the rough technology in the tooth construction might have been compensated in part by the lubrication. Thus, energy losses of the order of 10% or less may be reasonably conjectured.

References

[1] Pastore G. *Il Planetario di Archimede Ritrovato* (The Discovery of Archimedes' Orrery). © Copyright 2006-2010 - Giovanni Pastore, www.giovannipastore.it, ISBN 9788890471520 (in Italian).
[2] De Solla Price D.J. An ancient Greek computer. Scientific American, 200 (6):60-67, 1959.
[3] De Solla Price D.J. Gears from the Greeks. The Antikythera Mechanism: A Calendar Computer from ca. 80 B. C. Transactions of the American Philosophical Society, new series, 64(7):1–70, 1974.
[4] Wright M.T., Bromley A.G. and Magkou E. Simple X-ray Tomography and the Antikythera Mechanism. PACT. *Revue du groupe européen d'études pour les techniques physiques, chimiques, biologiques et mathématiques appliquées à l'archéologie* (Journal of the European Study Group on Physical, Chemical, Biological and Mathematical Techniques Applied to Archaeology), 45:531–543, 1995.
[5] The Antikythera Mechanism Research Project, http://www.antikythera-mechanism.gr. March 23, 20.